Int. J. Heat Mass Transfer. Vol. 24, pp. 181–183
Pergamon Press Ltd. 1981. Printed in Great Britain

0017–9310/81/0101–0181 $02.00/0

SHORTER COMMUNICATIONS

EXPONENTIALLY VARYING INTERNAL HEAT GENERATION IN FULLY-DEVELOPED, LAMINAR, RECTANGULAR CHANNEL FLOW

AVRAM BAR-COHEN
Department of Mechanical Engineering, Ben Gurion University, Beer Sheva, Israel

(*Received* 3 *December* 1979)

NOMENCLATURE

b, RF attenuation factor;
$\bar{b}$, nondimensional attenuation factor, by_0;
c, thermal coefficient of absorption;
$\bar{c}$, nondimensional thermal coefficient of absorption, $\frac{I_1 by_0^2}{k}c$;
c_p, specific heat;
I_1, RF power incident at surface 1;
I_l, RF power incident at location l;
k, thermal conductivity;
l, distance from surface 1;
T, temperature;
$\bar{T}$, nondimensional temperature, $\frac{k}{I_1 by_0^2}T$;
T_m, mean temperature;
T_1, temperature at surface 1;
T_{ml}, mean temperature over distance l from surface 1;
$\bar{V}$, nondimensional fluid velocity, $\frac{\rho c y_0}{k}V_m$;
V_m, mean fluid velocity;
V, x direction fluid velocity;
W, volumetric heat generation rate;
x, direction parallel to surface 1;
$\bar{x}$, nondimensional length, x/y_0;
y, direction perpendicular to surface 1;
$\bar{y}$, nondimensional length, y/y_0;
y_0, channel half width.

Greek symbols
α', RF attenuation factor;
ρ, fluid density.

INTRODUCTION

THE THERMAL consequences of heat generation in flowing liquids is of importance in the design and optimization of diverse systems including nuclear reactors as well as high power electromagnetic transmission circuits. Much of the literature in this field deals with constant or axially varying internal heat sources and only a limited number of reported studies have examined the effects of more complex heating functions, e.g. [1, 2]. In particular, scant attention has been paid to exponentially varying heat generation functions of the type encountered in the irradiation of fluids by electromagnetic energy beams.

This application category is epitomized by energy sinks or so-called 'water loads' in high power microwave systems where RF energy is beamed directly into a liquid stream flowing past an RF transparent surface. The interaction of the liquid molecules with the electric field results in the dissipation of the microwave energy and the local generation of heat in the fluid. Material and electrical constraints, pertinent to such an energy sink, dictate a maximum channel wall temperature and often require that no boiling occur in the fluid. As a result, a precise knowledge of the temperature profile in the fluid and especially along the channel wall is often crucial to the success of such systems.

Under a wide variety of conditions, the volumetric heat dissipation function associated with the liquid–RF interaction decreases exponentially from the transparent wall of the liquid channel and, with the nomenclature of Fig. 1, is expressible as

$$W_l = 0.23\,\alpha' I_1 \exp(-0.23 l \alpha'_{m,l}). \tag{1}$$

The attenuation factor, α', in itself a strong function of temperature and frequency [3] but over a modest temperature range and at a fixed electromagnetic frequency can be represented exponentially as $\alpha' = b\,e^{-CT}$.

Introducing this relation into equation (1), the internal heat generation rate is given by

$$W_l = (0.23\,b\,e^{-CT})(I_1\,e^{-0.23lb\,e^{-CT_{m,l}}}) \tag{2}$$

where it is to be noted that W_l is dependent on both the local temperature T and the average fluid temperature across the path length l, i.e. $T_{m,l}$.

THERMOFLUID FORMULATION

By appropriate simplification of the Navier–Stokes (Momentum Conservation) equations for fully-developed, constant property laminar flow between stationary parallel surfaces, it is possible to obtain the well known laminar velocity profile, e.g. [4]:

$$V = \frac{3}{2}V_m[1 - (y/y_0)^2]. \tag{3}$$

The general differential energy equation, which relates the rate of temperature increase of a fluid element moving in a stream to the heat conducted across its boundaries and

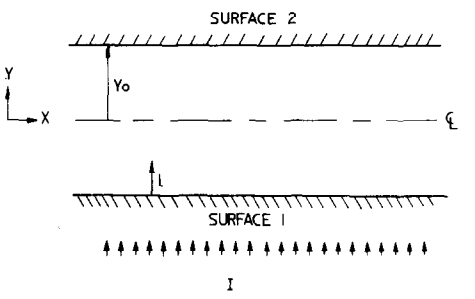

FIG. 1. Coordinate system for irradiated channel.

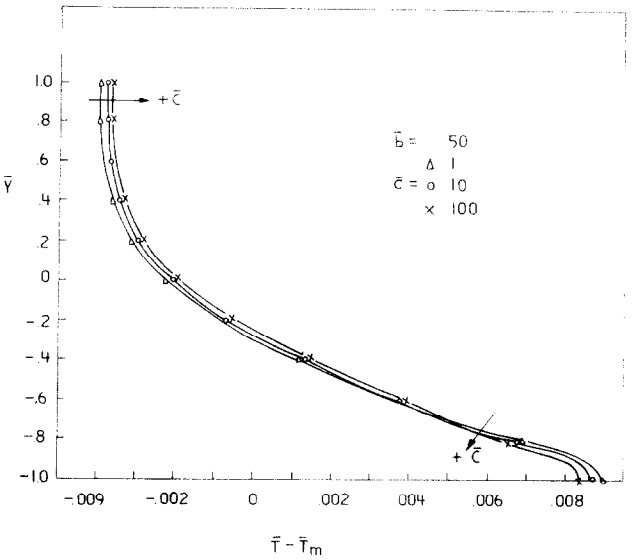

FIG. 2. Temperature profiles for irradiated channel, $\bar{b} = 50$, $\bar{c}$ varying.

internally generated, for two-dimensional steady state, fully-developed flow in a rectangular channel, can be expressed as

$$k\left(\frac{\partial^2 T}{\partial x^2}+\frac{\partial^2 T}{\partial y^2}\right)-\frac{3}{2}V_m[1-(y/y_0)^2]\rho c_p\frac{\partial T}{\partial x}=-W. \quad (4)$$

The expression for W, equation (2), with l replaced by y_0+y (see Fig. 1) can now be inserted to complete the formulation of the energy equation, i.e.

$$k\left(\frac{\partial^2 T}{\partial x^2}+\frac{\partial^2 T}{\partial y^2}\right)-\frac{3}{2}V_m[1-(y/y_0)^2]\rho c_p\frac{\partial T}{\partial x}$$
$$=-(0.23\,I_1\,b\,e^{-CT})(e^{-0.23(y_0+y)be+(y)be^{-CT_m,y_0+y}}) \quad (5)$$

With the exception of the radiationally opaque and near transparent limits, discussed in the next section, equation (5) is not easily amenable to solution and numerical techniques must be used. To maximize the utility of the solution, equation (5) can be non-dimensionalized by defining the following parameters:

$$\bar{V}=\rho c_p y_0 V_m/k \qquad \bar{X}=X/y_0$$
$$\bar{T}=kT/bI_1y_0^2 \qquad \bar{Y}=y/y_0 \quad (6)$$
$$\bar{C}=I_1by_0^2C/k \qquad \bar{b}=y_0b.$$

Introducing these parameters into equation (5), the energy equation takes the form.

$$\frac{\partial^2\bar{T}}{\partial\bar{X}^2}+\frac{\partial^2\bar{T}}{\partial\bar{y}^2}-\frac{3}{2}\bar{V}(1-\bar{y}^2)\frac{\partial\bar{T}}{\partial\bar{X}}$$
$$=-(0.23\,e^{-\bar{C}\bar{T}})(e^{0.23\bar{b}(1+\bar{y})e^{-\bar{C}\bar{T}_m,\bar{y}}}). \quad (7)$$

An interactive computer program for solving elliptic boundary value problems [5] was used interactively to generate the temperature fields defined by the solution of equation (7).

TEMPERATURE PROFILES

a. *Numerical solution*

The non-dimensional temperature, $\bar{T}$, in equation (7) can be seen to depend on the non-dimensional distance, $\bar{y}$, attenuation factor, $\bar{b}$ and the thermal coefficient of attenuation, $\bar{c}$. Consequently, the temperature profiles across the channel, i.e. $\bar{T}(\bar{y})$, were calculated for pre-determined values of $\bar{b}$ and $\bar{c}$, spanning the parametric range of interest. Figure 2 highlights the influence of $\bar{c}$ on the temperature profile and reveals that this parameter has only a marginal influence on $\bar{T}$ in the channel. Alternately, as can be seen in Fig. 3, both the temperature profile and the surface temperature are sensitive to the value of the dimensionless attenuation factor, $\bar{b}$.

b. *Opaque limit*

The form of the heat generation function, equation (2), suggests that two simple limits can be established for the temperature profile in the channel. At one limit, corresponding to very high values of b (or $\bar{b}$), the heat generation rate is strongly asymmetric and W falls rapidly with increasing distance from the RF beam entry surface. An upper limit on the surface temperature can thus be obtained by assuming the fluid to be radiationally opaque and all heat generation to occur in a vanishingly thin fluid layer or essentially at the channel wall.

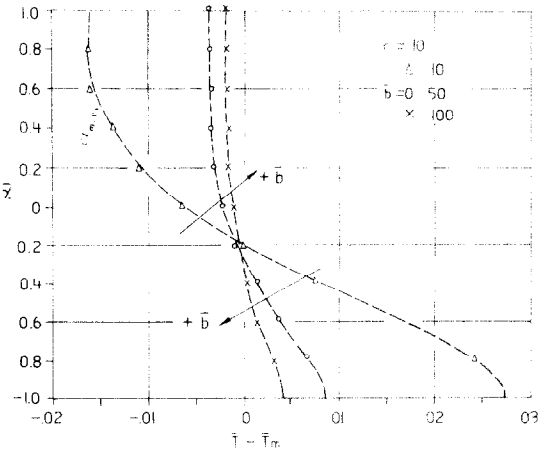

FIG. 3. Temperature profiles for irradiated channel, $\bar{c} = 10$, $\bar{b}$ varying.

Solution of the energy equation, equation (4), with $W = 0$ and $(\partial T/\partial y)_{-y_0} = I_1/k$, yields the temperature profile

$$T - T_m = \frac{I_1 y_0}{k}\left[\frac{y}{y_0} + \frac{3}{4}\left(\frac{y}{y_0}\right)^2 - \frac{1}{8}\left(\frac{y}{y_0}\right)^4 - 0.145\right]. \quad (8)$$

Solving equation (8) for the wall temperature and re-expressing this relation in terms of the non-dimensional parameters, the opaque limit on $\bar{T}_1 - \bar{T}_m$ is found as $(\bar{T}_1 - \bar{T}_m)_{\text{opaque}} = 1.74/\bar{b}$.

c. *Near transparent limit*

For low values of b (or $\bar{b}$) the fluid is nearly transparent and only mildly attenuates the incident radiation. Consequently, if the second channel wall is also RF transparent, the radiation traversing the channel will result in nearly uniform heat generation. If, on the other hand, the channel walls are internally reflective, the radiation arriving at surface 2 will be reflected back towards surface 1 and the entering radiation will eventually (following many multiple reflections) be absorbed nearly uniformly in the fluid.

Returning to equation (4) and setting W equal to a constant, $W = I_1/2y_0$, the channel temperature profile is found as

$$T - T_m = \frac{I_1 y_0}{k}\left[\frac{1}{8}\left(\frac{y}{y_0}\right)^2 - \frac{1}{16}\left(\frac{y}{y_0}\right)^4 - 0.0196\right]. \quad (9)$$

In addition to serving as a convenient limiting expression, equation (9) was used to check the accuracy of the numerical solution. One hundred iterations on a relatively coarse nodal matrix, of 11 nodes across and 20 nodes along the channel wall, yielded less than 8% discrepancy between the numerical solution and analytical values calculated at the nodal points. Since the number of iterations is proportional to the number of nodes, the above nodal matrix was employed in all the numerical calculations.

Solving equation (9) for $y = y_0$ and re-expressing in terms of the dimensionless parameters, the lower near-transparent limit on the wall temperature is found as $(\bar{T} - \bar{T}_m)_{\text{transport}} = 0.0428/\bar{b}$.

The two limiting equations for $(\bar{T}_1 - \bar{T}_m)$ are plotted in Fig. 4 and are seen to properly bound the numerically calculated values of the dimensionless wall-to-mean fluid temperature difference. However, the factor of approximately 18 separating the lower and upper limits on $(\bar{T}_1 - \bar{T}_m)$ suggests that for all but extreme values of $\bar{b}$, i.e. $\bar{b} \ll 1$ or $\bar{b} \gg 100$, the numerical results must be used to determine the desired temperature.

d. *General considerations*

Due to the particular choice of non-dimensionalizing parameter, increasing attenuation, i.e. higher $\bar{b}$ values, results in smaller values of $\bar{T}_1 - \bar{T}_m$. However, a review of the pertinent equations shows that, as anticipated, increasing b leads to a progressively larger temperature difference, $T_1 - T_m$, as the solutions approach the radiationally opaque limit.

Emphasis throughout this discussion has been placed on the temperature profile, relative to the mean liquid temperatures in the channel. The reader is reminded that for an axially-invariant heating function, the axial gradient equals

$$dT_m/dX = I_1/2\rho c_p y_0 V_m. \quad (10)$$

Consequently, once the inlet liquid temperature is known, equation (10) suffices to calculate T_m at every location in the channel.

Acknowledgements — The author is indebted to D. L. Cochran and B. B. Mikic for their aid in the formulation of the 'water load' problem.

REFERENCES

1. A. L. Loeffler, Jr., Heat transfer in fully developed flow between parallel plates with variable heat sources, *Nucl. Sci. Engng* **2**, 547–567 (1957).
2. L. Topper, Heat transfer in cylinders with heat generation, *A. I. Ch. E. Jl* **1**, 463–466 (1955).
3. A. Von Hippel, The dielectric relaxation spectra of water, ice and aqueous solutions and their interpretation, Technical Report II, Laboratory for Insulation Research, MIT, Cambridge, Mass (1967).
4. W. M. Rohsenow and H. Choi, *Heat, Mass and Momentum Transfer*, Prentice Hall, Englewood Cliffs, NJ (1961).
5. C. C. Tillman, Jr., EPS: An interactive system for solving elliptic boundary value problems, MIT report MAC-TR-62, Cambridge, Massachusetts (1969).

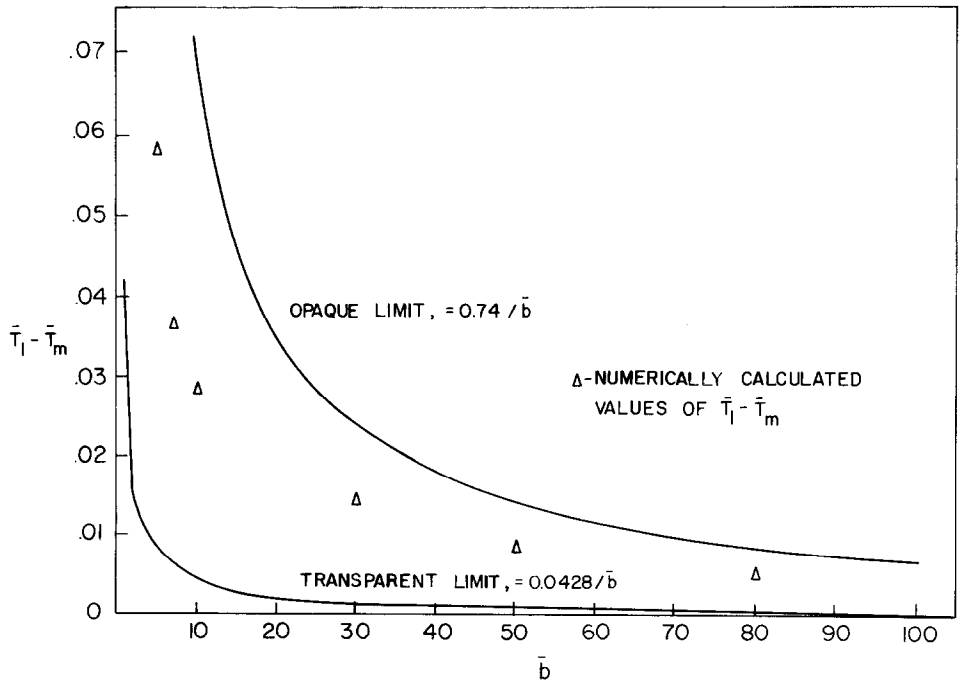

FIG. 4. Surface temperature dependence on $\bar{b}$.